Infrared studies of the normal and superconducting states of $Y_1Ba_2Cu_3O_7$

by R. T. Collins
Z. Schlesinger
F. H. Holtzberg
P. Chaudhari
C. A. Feild

We describe infrared measurements of the *a–b*-plane response of $Y_1Ba_2Cu_3O_7$ crystals with $T_c \simeq 92$ K. We observe a self-energy structure at a characteristic energy of 500 cm^{-1} ($8kT_c$), the appearance of which coincides with the transition to the superconducting state. The nature of this self-energy anomaly is consistent with its identification as a nodeless *a–b*-plane energy gap at $2\Delta \simeq 8kT_c$. On the basis of temperature-dependent measurements above T_c, we suggest that the normal state can be primarily characterized by a carrier band with an enhanced low-frequency mass and a frequency-dependent scattering rate. Our data indicate that these arise from coupling to an excitation spectrum with characteristic frequencies up to $\omega_c \sim 700$ cm^{-1} and a coupling strength of $\lambda \simeq 2$–3.

Introduction

The recent discovery of high-temperature superconductivity in layered copper-oxide compounds [1, 2] has been followed by a monumental effort to understand the physics of these systems. Crucial to that endeavor is the reliable measurement of fundamental properties in both the normal and superconducting states. Spectroscopic techniques, such as inelastic neutron scattering, tunneling, and infrared spectroscopy, are particularly important because they probe the spectrum of intermediate-energy (i.e., 1 meV to 1 eV) excitations, which are presumably crucial to the mechanism of high-temperature superconductivity.

Early controversies in the infrared work resulted from attempts to draw conclusions from data from polycrystalline samples. For example, an unusually small reduced-energy gap, $2\Delta \simeq 2.5kT_c$, was inferred from measurements of polycrystalline $La_{2-x}Sr_xCuO_4$ samples [3–5]. Subsequently Bonn et al. [6] proposed that the existence of an extremely low-energy plasma edge obscures the energy gap, while Schlesinger et al. [7] found that, because of the large anisotropy, the gap measurement on unoriented polycrystalline samples is especially sensitive to the out-of-plane (c-axis) response. Whether there actually is a low-energy plasma edge or a small energy gap associated with a

particular direction in this anisotropic material [7, 8] is not resolved; however, it is clear that because of anisotropy, definitive conclusions regarding $2\Delta/kT_c$ cannot be drawn from data on polycrystalline samples.

In the normal state the existence of an enormous peak in $\sigma(\omega)$ at about 0.5 eV was inferred from room-temperature reflectivity measurements on polycrystalline samples [9–11]. The behavior of the reflectivity seemed similar to that previously observed in cubic $BaPb_{1-x}Bi_xO_3$ [12], where the existence of a mid-infrared absorption was inferred from a small deficit in the reflectivity below the plasma edge. The corresponding reflectivity deficit in $La_{2-x}Sr_xCuO_4$ and $Y_1Ba_2Cu_3O_7$ was much larger. This large reflectivity deficit was subsequently shown to be primarily associated with anisotropy in the layered Cu oxides [7], and thus does not constitute evidence for the existence of a mid-infrared mode. Specifically, for polycrystalline samples, contributions to the reflectivity associated with the out-of-plane (c-axis) response enter the overall reflectivity in such a way as to make any conductivity determination quite unreliable.

Current controversies regarding the infrared work involve much more subtle disagreements on the interpretation of generally valid data from crystalline samples. From the first far-infrared measurements on crystals, Schlesinger, Collins, et al. [13] reported an energy gap associated with the a–b-plane response of $Y_1Ba_2Cu_3O_7$ of $2\Delta \simeq 8kT_c$. This conclusion was based on measurements of reflectivity ratios which show a peak consistent with the occurrence of a nodeless energy gap at 500 cm^{-1} ($8kT_c$) [13, 14]. Although data consistent with the original measurement of Schlesinger, Collins, et al. [13] have been independently obtained by several other groups, the evidence for an $8kT_c$ gap has been questioned by Bonn et al. [15], who suggested that the gap may be obscured by a plasma edge, and by Thomas et al. [16], who have reported a gap of $2\Delta \simeq 3.5kT_c$ for their oxygen-deficient samples, and have suggested that the structure at $8kT_c$ is merely a continuation of normal-state temperature dependence. In this paper we present further evidence supporting our original point of view [13, 14], including temperature-dependent data which show that the onset of our $8kT_c$ reflectivity enhancement coincides with T_c, and is thus not the continuation of normal-state temperature dependence as suggested by Thomas et al. Our results show that there is clearly a self-energy anomaly at $8kT_c$ (500 cm^{-1}) associated with the superconducting state, and strongly suggest the identification of this self-energy structure as a nodeless a–b-plane energy gap. A reconciliation of our large energy gap with the much smaller one of Thomas et al. [16] may be achievable when the effects of the anisotropy between the a–b plane and the c-axis direction are considered.

The central question regarding the normal-state infrared properties is whether the conductivity of the copper–oxygen planes is most appropriately described in terms of a dynamic interaction which leads to a frequency-dependent scattering rate and carrier mass or as a superposition of a free-carrier band and some type of mid-infrared interband transition [15]. These two approaches differ fundamentally, since the former implies a strongly coupled normal state, while the latter is most consistent with a weak-coupling view. In this work we describe reflectivity measurements on the a–b plane of $Y_1Ba_2Cu_3O_7$ crystals and films with transitions at $T_c \simeq 92$ K. We find that either model can describe the reflectivity at a single temperature, but, in contrast with similar work on oxygen-deficient material [16], we find significant temperature dependence in $R(\omega)$ and $\sigma(\omega)$ through the crucial mid-infrared region [17]. This broad-band temperature dependence is inconsistent with a mid-infrared band model, and suggests the need for frequency-dependent scattering in order to understand the normal-state infrared behavior.

Experimental procedures

Our measurements were made on the a–b plane of oriented films of $Y_1Ba_2Cu_3O_7$ with relatively large areas ($\simeq$10 mm^2) and on crystals of smaller area ($\simeq$2 mm^2), with both as annealed and polished surfaces. The films were grown on $SrTiO_3$ substrates to a thickness of $\sim$1 μm. Both films and crystals were single-phase. The samples are micro-twinned, so that an average of the a–b-plane properties is obtained. ac susceptibility measurements showed the samples to have superconducting transitions at $\sim$92 K, with widths of less than 0.2 K for the crystals and of $\sim$1 K for the films. Reflectivity measurements were made at near-normal incidence. Each sample was mounted in close proximity to an evaporated gold reference mirror which was carefully aligned parallel to the sample surface. A manipulator allowed either the sample or reference to be positioned in the infrared beam. We tested our technique by studying both brass–Au and Au–Au reflectivity ratios, and in each case obtained a precision of better than one percent.

Results

In **Figure 1** the ratio of the reflectivity in the superconducting state ($T = 40$ K) to that in the normal state ($T = 95$ K) is shown. From this measurement, one can see that below about 600 cm^{-1} the reflectivity in the superconducting state is higher than that in the normal state. This reflectivity ratio R_s/R_n has a maximum value of about 3% at about 470 cm^{-1} ($8kT_c$) and then drops rapidly with increasing frequency and exhibits a minimum near 800 cm^{-1}. It is important to show that this reflectivity enhancement is associated with the transition to superconductivity; therefore, in **Figure 2(a)** we plot $R(T)/R(95\text{ K})$ for several temperatures in the neighborhood of T_c. We observe that the changes in $R(T)/R(95\text{ K})$ occur primarily between 90 and 60 K, i.e., just below T_c. The relationship between T_c and our reflectivity enhancement is

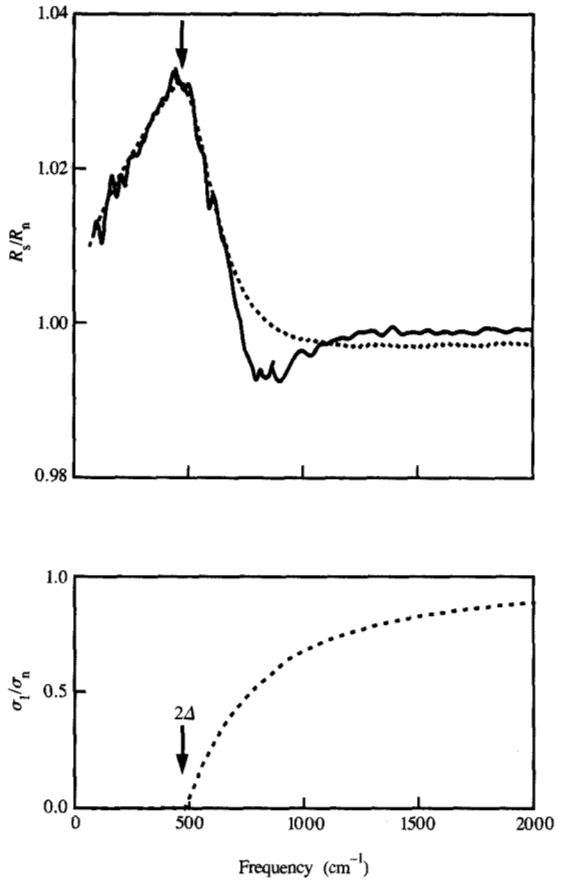

Figure 1

The ratio of the a–b-plane reflectivity in the superconducting state (40 K) to that in the normal state (T = 92 K) as measured on twinned crystals (T_c = 92 K) is shown along with a Mattis–Bardeen fit (dotted line) to the data. The ratio is independent of temperature below about 50 K. In the lower section the real part of the Mattis–Bardeen conductivity ratio σ_1/σ_n is shown for a gap of 2Δ = 480 cm^{-1}.

further illustrated in **Figure 2(b)**, which shows the amplitude of the reflectivity enhancement as a function of temperature. This amplitude shows a clear onset at T_c, and very little change above T_c in the normal state.

In an ordinary s-wave superconductor R_s/R_n is peaked at 2Δ, as shown by the dotted curve in Figure 1(a), which is based on a calculation using the Mattis–Bardeen form for the conductivity in the superconducting state [14, 18]. The presence of a distinct peak in the measured R_s/R_n and the reasonable agreement with the Mattis–Bardeen peak suggest the occurrence of a nodeless $8kT_c$ energy gap in the a–b plane. This energy scale is much larger than observed in other superconductors, including $BaPb_{1-x}Bi_xO_3$ and $Ba_{1-x}K_xBiO_3$, where reduced gaps of $2\Delta \simeq 4kT_c$ have been observed using the same experimental method [19, 20].

We have measured the normal-state reflectivity of our samples for temperatures between 300 K and 95 K. In **Figure 3** we show spectra taken at 250 K (dots) and 100 K (triangles) for a polished face of one of our $Y_1Ba_2Cu_3O_7$ crystals. We see in Figure 3 that the reflectivity increases

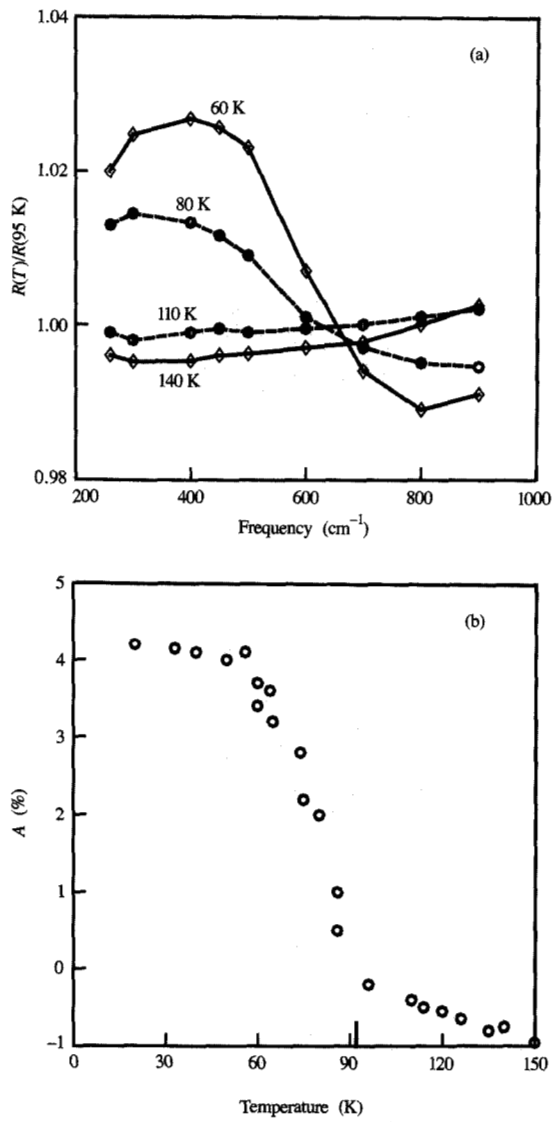

Figure 2

(a) The reflectivity ratio $R(T)/R(T = 95\ K)$ is shown for T = 60, 80, 110, and 140 K. (b) The amplitude of the reflectivity enhancement is plotted vs. T, demonstrating a clear onset at T_c for our $8kT_c$ reflectivity enhancement. $A(T)$ is defined as the difference between $R(T)/R$ (95 K) at 400 cm^{-1} and 800 cm^{-1}.

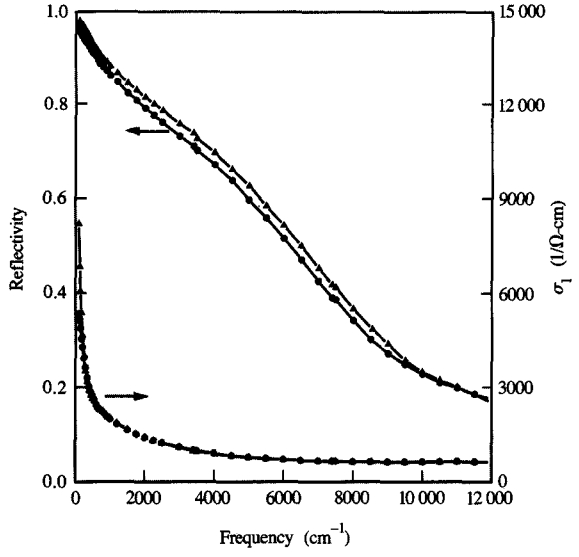

Figure 3

The reflectivity and the real part of the conductivity of $Y_1Ba_2Cu_3O_7$ are shown for T = 100 K (triangles) and 250 K (dots) for ω up to 12000 cm^{-1}.

over a very wide frequency range (~100 cm^{-1} to 8000 cm^{-1}) as T is reduced in the normal state. Virtually identical spectra were observed for as-annealed crystal faces. Although the films showed a slightly lower reflectivity (~5% lower at 4000 cm^{-1}) in the mid-infrared, they displayed the same temperature dependence as observed for the crystal samples. All of the samples discussed here exhibited a distinct gap-like increase in low-frequency reflectivity with an onset at T_c and a characteristic energy scale of 7–8kT_c, as shown in Figures 1 and 2 and as we have previously reported [13, 14].

Figure 3 also gives the real part of the conductivity, $\sigma_1(\omega)$, at 250 K and 100 K, obtained by a Kramers–Kronig transform of the reflectivity [17]. We obtain the plasma frequency from the f-sum rule on $\sigma_1(\omega)$, which we integrate up to ~20 000 cm^{-1} after subtracting a temperature-independent interband (Lorentz oscillator) contribution to $\sigma_1(\omega)$ centered at ~2 eV. In this manner a plasma frequency of $\omega_p \simeq 22\,000$ cm^{-1} $\simeq$ 2.7 eV is obtained, corresponding to a ratio

$$\frac{n}{m_b} \simeq \frac{5.5 \times 10^{21}\ \text{cm}^{-3}}{m_e},$$

where n is the free-carrier concentration and m_b is the band mass, in agreement with previous results [13, 14].

In **Figure 4**, the reflectivity (from Figure 3) and the real [$\sigma_1(\omega)$] (a) and imaginary [$\sigma_2(\omega)$] (b) parts of $\sigma(\omega)$ are plotted

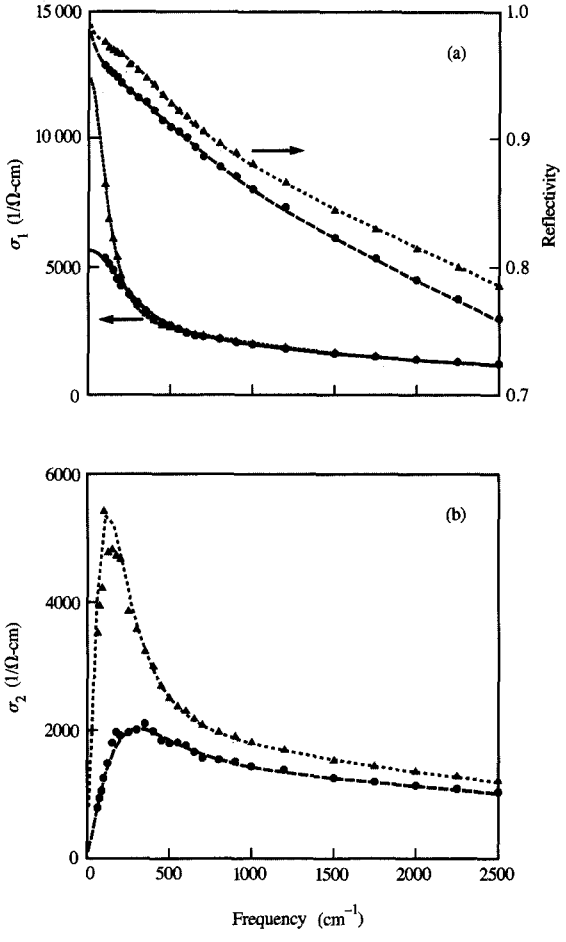

Figure 4

The reflectivity and the real part of the conductivity of $Y_1Ba_2Cu_3O_7$ (a) and the imaginary part of the conductivity (b) are shown for T = 100 K (triangles) and 250 K (dots) for ω up to 2500 cm^{-1}. The lines through the data points refer to a frequency-dependent scattering model calculation described in the text.

for $\omega < 2500$ cm^{-1}. We can analyze the conductivity in terms of a frequency-dependent scattering model in which

$$\tilde{\sigma}(\omega) = \frac{ne^2\tau^*(\omega)}{m^*(\omega)[1 - i\omega\tau^*(\omega)]}, \qquad (1)$$

where $m^*(\omega) = m_b[1 + \lambda(\omega)]$ is the renormalized mass, and $\tau^*(\omega) = \tau(\omega)[1 + \lambda(\omega)]$ is the renormalized scattering rate. Frequency-dependent scattering models have previously been used to treat electron–phonon interactions in ordinary metals [21] and spin-related excitations in heavy Fermion systems [22, 23].

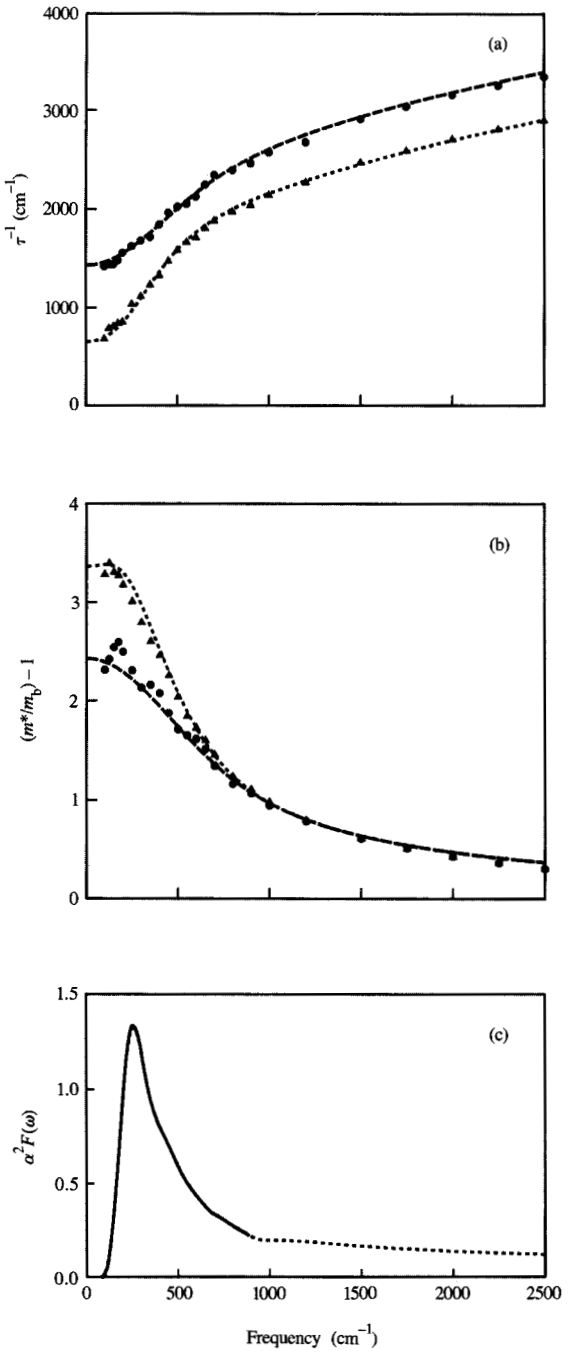

Figure 5

The unrenormalized scattering rate (a) and the reduced mass enhancement (b) of $Y_1Ba_2Cu_3O_7$ are shown for $T = 100$ K (triangles) and 250 K (dots). The lines through the data points in (a) and (b) refer to a model calculation which uses the coupling spectrum, $\alpha^2F(\omega)$, shown in (c).

In **Figure 5** we plot $\tau^{-1}(\omega)$ and $(m^*/m_b) - 1$, which are obtained using Equation (1) with

$$\frac{n}{m_b} = \frac{5.5 \times 10^{21}\ \text{cm}^{-3}}{m_e},$$

and, like $\sigma_1(\omega)$ and $\sigma_2(\omega)$, are related by causality. The behavior shown in Figures 5(a) and 5(b) can be understood as a consequence of an interaction of the charged carriers with an inelastic scattering spectrum. At low temperature and frequency the carriers have an enhanced mass because they drag an excitation cloud along with them, and the scattering rate is low since the inelastic scattering channels are not energetically available. With increasing frequency, the scattering rate increases as additional scattering channels become accessible, and the mass enhancement diminishes as the carriers shed their excitation cloud. In this manner an excitation spectrum which is not itself infrared active, but which is strongly coupled to the carriers, can dramatically influence the infrared (and dc) conductivity. In Figure 5 the frequency dependence of $\tau^{-1}(\omega)$ is most rapid from about 200–700 cm^{-1}. Within the inelastic scattering approach, we associate this with the characteristic frequency of the excitation spectrum to which the carriers are coupled. The low frequency value of $\lambda(\omega)$ at 100 K indicates an overall coupling strength of roughly $\lambda = 3$ to that spectrum. This coupling strength lies between that typical of the electron–phonon interaction ($\lambda \simeq 1$) and the very large values associated with "spin-fluctuation-exchange"-induced mass enhancements ($\lambda \simeq 50$) in moderately heavy electron systems such as UPt_3 and $CePd_3$ [22, 23].

In our frequency-dependent scattering analysis of the conductivity, we have assumed only a single free-carrier band. The low-frequency peak in $\sigma_1(\omega)$ in the 100 K conductivity is a direct consequence of the reduced scattering rate at frequencies less than the characteristic scattering energy. Bonn et al. [15] have suggested an alternative analysis of the *a*–*b*-plane conductivity in which $\sigma_1(\omega)$ is divided into a low-frequency Drude peak with a frequency-independent scattering rate and a temperature-independent interband transition which is responsible for the mid-infrared conductivity. We are able to fit this mid-infrared band model to our 100 K spectrum (with approximately 1/4 of the area in the low-energy peak); however, we find that the temperature dependence predicted by the model is inconsistent with our observations. In particular, neither $R(\omega)$ nor $\sigma(\omega)$ is predicted to show temperature dependence for $\omega \gtrsim 1000$ cm^{-1} (in the part of the spectrum dominated by the interband transition). In a frequency-dependent scattering model there is a fundamental relationship between frequency and temperature dependence. To illustrate this, it is useful to introduce a coupling spectrum, $\alpha^2F(\omega)$, from which a scattering rate and mass enhancement are calculated as a function of frequency and temperature. In general, this is a

nontrivial calculation that requires a detailed knowledge of the nature of the interaction. Here, for the sake of simplicity, we approximate the optical scattering rate, $\tau^{-1}(\omega)$, by the quasi-particle lifetime averaged over the Fermi surface, and use [24]

$$\tau^{-1}(\omega) = -2\,\mathrm{Im}\,\Sigma(\omega) = \pi \int_0^\infty d\omega' \alpha^2 F(\omega') f(\omega';\, T), \qquad (2)$$

where $\Sigma(\omega)$ is the self-energy and

$$f(\omega';\, T) = \coth\frac{\omega'}{2T} - \frac{1}{2}\tanh\frac{\omega' + \omega}{2T} - \frac{1}{2}\tanh\frac{\omega' - \omega}{2T}$$

is an occupation-factor-related term which contains all of the temperature dependence in Equation (2). Figure 5(c) shows a spectral function which provides a fit to both the temperature and frequency dependence of our data [dashed (250 K) and dotted (100 K) curves] in Figures 4 and 5. [$(m/m_b) - 1$ is obtained from a Kramers–Kronig transform of $\tau^{-1}(\omega)$.] We have included an elastic contribution to $\tau^{-1}(\omega)$ of 560 cm^{-1}. The spectral function $\alpha^2 F(\omega)$ obtained by this fitting procedure should be viewed only as a rough approximation to the true coupling spectrum. In particular, calculations which explicitly take into account the difference between the transport scattering rate and quasi-particle lifetime indicate that the spectral weight above 800 cm^{-1} should be ignored [25]. The integrated coupling strength in this high-frequency range is less than 1, and hence does not dramatically alter our estimate of the total coupling. These calculations also predict a somewhat larger temperature dependence than we observe. The salient point is that the temperature dependence exhibited by our data is qualitatively consistent with the presence of frequency-dependent scattering rather than with the mid-infrared-mode model. We cannot rule out the possibility that frequency-dependent scattering and a mid-infrared mode may both be present. This is a particularly interesting possibility in $Y_1Ba_2Cu_3O_7$, where the presence of localized carriers on the chains could give a mode-like contribution to the mid-infrared. Reflectivity measurements in the near-infrared (>8000 cm^{-1}) already indicate that the *a*-axis and *b*-axis are inequivalent [26]. Separation of the *a*–*b*-plane conductivity into chain and plane contributions will have to wait for studies of untwinned samples. At present we do not feel that the contributions of the chains will significantly alter the mass enhancement ($\lambda \simeq 2$–3) or characteristic scattering frequency (<700 cm^{-1}) obtained in our present analysis of data from twinned samples.

In models of transport in correlated systems potentially applicable to $Y_1Ba_2Cu_3O_7$, a mass enhancement can arise from the interaction of the carriers with spin-related excitations associated with the Cu, for which the characteristic energy scale is set by the exchange interaction, *J*. (In RVB language, this is the holon–spinon scattering.) For example, Kane et al. [27] have studied the motion of a hole in a large-*U* Hubbard model with either Néel or an RVB order, and have obtained a mass enhancement of order t/J associated with coupling to spin excitations of characteristic energy *J*, where $4t$ is the hole bandwidth. In principle, strong electron–phonon coupling provides an alternative origin for our measured mass enhancement (the phonon density of states is roughly constant up to a cutoff frequency of about 600 cm^{-1} [28]). The observed overall coupling strength, $\lambda \sim 2$–3, however, would be unprecedented, particularly at such a high-frequency scale.

In Figure 5 we have plotted $\tau^{-1}(\omega)$; however, the actual (renormalized) scattering rate is $\tau^{*-1}(\omega) = \tau^{-1}(\omega) m_b/m^*$. It is interesting to note that throughout our frequency range the inelastic contribution to $\hbar/\tau^{*-1}(\omega)$ is of order $kT + \hbar\omega$, suggesting a nearly localized Fermi liquid, or that $Y_1Ba_2Cu_3O_7$ is at the edge of the regime in which a Fermi liquid theory is well defined.

An examination of the correspondence between our infrared results and other measurable quantities is also useful. For example, using our measured values for ω_p and m^*/m_b, we estimate the *a*–*b*-plane London penetration depth to be $\lambda = c/\omega_p(m^*/m_b)^{1/2} \simeq 1400$ Å. Specific heat measurements are also expected to exhibit the same mass enhancement as with the infrared. The correspondence between our infrared data and the dc conductivity can be examined using the measured low-frequency values of $\tau^{-1}(\omega)$ [Figure 3(a)] in the $\omega = 0$ limit of Equation (1), $\sigma_{dc} = ne^2\tau(0)/m_b$, from which we obtain 85, 105, 140, and 175 $\mu\Omega$-cm at $T = 100$, 150, 200, and 250 K, respectively. These values are comparable to typical measured dc resistivities on similar crystals. Although they appear to extrapolate roughly to the origin, there is actually some upward curvature, which in the model leads to a positive intercept on the *y*-axis.

Efforts to measure and interpret the *a*–*b*-plane infrared conductivity of crystalline $Y_1Ba_2Cu_3O_7$ began with [13], in which $\sigma_1(\omega)$ at room temperature and $\omega \gtrsim 1000$ cm^{-1} were reported, and $\sigma_1(\omega)$ did not exhibit the very strong 0.3–0.5-eV peak previously reported based on data from polycrystalline samples. Subsequent efforts extended this work to lower frequencies and temperatures [15, 16], where Bonn et al. [15] first showed evidence for a temperature-dependent peak in $\sigma_1(\omega)$ (as shown in Figure 4) which allows the connection with σ_{dc} to be made. Sulewski et al. [29] were the first to apply a frequency-dependent scattering model to the oxide superconductors in their study of ceramic $Y_1Ba_2Cu_3O_7$. More recently, Thomas et al. [16] have analyzed the *a*–*b*-plane conductivity of O-deficient crystals ($T_c \simeq 50$–70 K) in terms of the frequency-dependent scattering model and have obtained a coupling of $\lambda \sim 9$, although, as they point out, their measured temperature dependence is not consistent with their carrier-oscillator model [16]. Our results are similar to theirs in terms of the frequency scale of coupling; however, for the coupling constant we obtain $\lambda \sim 3$. This substantial difference in the

coupling strength estimate for our 92 K crystals and their lower-T samples suggests a high degree of sensitivity of the normal-state behavior to the O content (or, alternatively, hole density.)

Conclusion

In conclusion, we find that the frequency and temperature dependence of the normal-state transport of $Y_1Ba_2Cu_3O_7$ in the far-infrared region supports a frequency-dependent scattering rate arising from coupling to an excitation spectrum with a characteristic energy cutoff of $\sim 700\ cm^{-1}$ and an integrated coupling strength of $\lambda \simeq 2$–3. This approach provides a unified description of the temperature and frequency dependence of the transport behavior above T_c. Below T_c a reflectivity enhancement with a distinct onset at the superconducting transition is observed to occur at a characteristic energy of $500\ cm^{-1}$ ($8kT_c$). The data clearly demonstrate the presence of a self-energy structure at $8kT_c$ in the superconducting state, and are consistent with the interpretation of this structure as a nodeless a–b-plane energy gap of $2\Delta \simeq 8kT_c$.

Acknowledgments

We would like to acknowledge excellent technical assistance from J. A. Calise, Gene Komsa, and John Sosik, and valuable conversations with P. W. Anderson, D. J. Scalapino, H. Fukuyama, P. A. Lee, D. M. Newns, A. J. Sievers, and B. C. Webb. Insights developed over the last decade in Sievers' group (which includes F. E. Pinkerton, B. C. Webb, and P. E. Sulewski) have been crucial to our present effort.

References

1. J. G. Bednorz and K. A. Müller, *Z. Phys. B* **64,** 189 (1986); J. G. Bednorz, M. Takashige, and K. A. Müller, *Europhys. Lett.* **3,** 379 (1987).
2. M. K. Wu, J. Ashburn, C. J. Torng, P. H. Hor, R. L. Meng, L. Gao, Z. J. Huang, Y. Q. Wang, and C. W. Chu, *Phys. Rev. Lett.* **58,** 908 (1987).
3. P. E. Sulewski, A. J. Sievers, R. A. Buhrman, J. M. Tarascon, and L. H. Greene, *Phys. Rev. B* **35,** 5330 (1987).
4. Z. Schlesinger, R. L. Greene, J. G. Bednorz, and K. A. Müller, *Phys. Rev. B* **35,** 5334 (1987).
5. U. Walter, M. S. Sherwin, A. Stacy, P. L. Richards, and A. Zettle, *Phys. Rev. B* **35,** 5327 (1987).
6. D. A. Bonn, J. E. Greedan, C. V. Stager, T. Timusk, M. Doss, S. Herr, K. Kamaras, C. Porter, D. B. Tanner, J. M. Tarascon, W. R. McKinnon, and L. H. Greene, *Phys. Rev. B* **35,** 8843 (1987).
7. Z. Schlesinger, R. T. Collins, M. W. Shafer, and E. M. Engler, *Phys. Rev. B* **36,** 5275 (1987).
8. R. T. Collins, Z. Schlesinger, R. H. Koch, R. B. Laibowitz, T. S. Plaskett, P. Freitas, W. J. Gallagher, R. L. Sandstrom, and T. R. Dinger, *Phys. Rev. Lett.* **59,** 704 (1987).
9. J. Orenstein, G. A. Thomas, D. H. Rapkine, C. G. Bethea, B. F. Levine, R. J. Cava, E. A. Rietman, and D. W. Johnson, Jr., *Phys. Rev. B* **36,** 729 (1987).
10. K. Kamaras, C. D. Porter, M. G. Doss, S. L. Herr, D. B. Tanner, D. A. Bonn, J. E. Greedan, A. H. O'Reilly, C. V. Stager, and T. Timusk, *Phys. Rev. B* **36,** 733 (1987).
11. D. A. Bonn, J. E. Greedan, C. V. Stager, T. Timusk, M. G. Doss, S. L. Herr, K. Kamaras, and D. B. Tanner, *Phys. Rev. Lett.* **58,** 2249 (1987).
12. S. Tajima, S. Ushida, A. Masaki, H. Tagaki, K. Kitazawa, S. Tanaka, and S. Sugai, *Phys. Rev. B* **35,** 696 (1987); S. Tajima, S. Ushida, A. Masaki, H. Tagaki, K. Kitazawa, S. Tanaka, and S. Katsui, *Phys. Rev. B* **32,** 6302 (1985).
13. Z. Schlesinger, R. T. Collins, D. L. Kaiser, and F. Holtzberg, *Phys. Rev. Lett.* **59,** 1958 (1987).
14. Z. Schlesinger, R. T. Collins, D. L. Kaiser, F. Holtzberg, G. V. Chandrashekhar, M. W. Shafer, and T. M. Plaskett, *Physica C* **153–155,** 1734 (1988).
15. D. A. Bonn, A. H. O'Reilly, J. E. Greedan, C. V. Stager, T. Timusk, K. Kamarás, and D. B. Tanner, *Phys. Rev. B* **37,** 1574 (1988); T. Timusk, S. L. Herr, K. Kamarás, C. D. Porter, D. B. Tanner, D. A. Bonn, J. D. Garrett, C. V. Stager, J. E. Greedan, and M. Reedyk, preprint.
16. G. A. Thomas, J. Orenstein, D. H. Rapkine, M. Capizzi, A. J. Millis, R. N. Bhatt, L. F. Schneemeyer, and J. V. Waszczak, preprint.
17. R. T. Collins, Z. Schlesinger, F. Holtzberg, P. Chaudhari, and C. Feild, preprint.
18. D. C. Mattis and J. Bardeen, *Phys. Rev.* **111,** 412 (1958).
19. Z. Schlesinger, R. T. Collins, B. A. Scott, and J. A. Calise, *Phys. Rev. B* **38,** 92 (1988).
20. Z. Schlesinger, R. T. Collins, J. A. Calise, D. J. Hinks, A. W. Mitchell, Y. Zheng, and B. Dabrowski, submitted to *Phys. Rev. Lett.*
21. P. B. Allen, *Phys. Rev. B* **3,** 305 (1971).
22. B. C. Webb, A. J. Sievers, and T. Mahalisin, *Phys. Rev. Lett.* **57,** 1951 (1986).
23. P. E. Sulewski, A. J. Sievers, M. B. Maple, M. S. Torikachvili, J. L. Smith, and Z. Fisk, *Phys. Rev. B*, to be published.
24. A. J. Millis, Subir Sachdev, and C. M. Varma, *Phys. Rev. B* **37,** 4975 (1988).
25. D. J. Scalapino, G. Bickers, Z. Schlesinger, and R. T. Collins, unpublished work; A. J. Millis, unpublished work.
26. M. P. Petrov, A. I. Grachev, M. V. Krasin'kova, A. A. Nechitailov, V. V. Prokofiev, V. V. Poborchy, S. I. Shagin, and N. F. Kartenko, *Solid State Commun.* **67,** 1197 (1988).
27. C. L. Kane, P. A. Lee, and N. Read, preprint.
28. B. Renker, E. Gering, G. Roth, W. Reichardt, D. Ewert, and H. Rietschel, preprint.
29. P. E. Sulewski, T. W. Noh, J. T. McWhirter, A. J. Sievers, S. E. Russek, R. A. Buhrman, C. S. Jee, J. E. Crow, R. E. Salomon, and G. Myer, *Phys. Rev. B* **36,** 2357 (1987).

Received January 6, 1989; accepted for publication February 2, 1989

Reuben T. Collins *IBM Research Division, T. J. Watson Research Center, P.O. Box 218, Yorktown Heights, New York 10598.*
Dr. Collins received a B.A. in physics and mathematics from the University of Northern Iowa, Cedar Falls, in 1979, and a Ph.D. in applied physics from the California Institute of Technology, Pasadena, in 1984, when he joined the research staff at the IBM T. J. Watson Research Center. Dr. Collins' research is primarily involved with the optical and electronic properties of semiconductors and superconductors, including inelastic tunneling and photoconductivity studies of semiconductor heterostructures and, more recently, infrared properties of high-temperature superconductors.

Zack Schlesinger *IBM Research Division, T. J. Watson Research Center, P.O. Box 218, Yorktown Heights, New York 10598.*
Dr. Schlesinger was an undergraduate at the University of California at Santa Barbara. At Cornell University he studied the propagation of infrared surface electomagnetic waves, receiving a Ph.D. in physics in 1981. While on a postdoctoral assignment at Bell Laboratories, he studied the far-infrared properties of two-dimensional electron layers at semiconductor interfaces. Since 1983, Dr. Schlesinger has been a Research Staff Member at the IBM T. J. Watson Research Center, where his current interests include the physics of conducting two-dimensional systems and high-temperature superconductors.

Frederic H. Holtzberg *IBM Research Division, T. J. Watson Research Center, P.O. Box 218, Yorktown Heights, New York 10598.*
Dr. Holtzberg received his Ph.D. from the Polytechnic University of New York in 1952 and joined IBM that year at the T. J. Watson Scientific Computing Center at Columbia University. In 1959 he was appointed Technical Assistant to the Special Assistant to the President of the United States for Science and Technology (on leave of absence from IBM) and Consultant to the Office of Science and Technology, Executive Office of the President. He returned to the Yorktown Research Center in 1960 to the director's staff. In 1966 he received an IBM Outstanding Contribution Award for his contributions in the field of rare-earth research. Dr. Holtzberg became a Fellow of the American Physical Society in 1975. He has been an adjunct professor at the University of Grenoble and has been appointed to the staff of the Centre d'Etudes Nucléaires de Grenoble. He has served as a group and a department manager in material sciences at the IBM Yorktown Research Center; in 1982 he resumed his interests in personal research. He was awarded an honorary degree by L'Université Scientifique Technologique et Médicale de Grenoble in 1987. Dr. Holtzberg's research interests include crystal chemistry, X-ray crystallography, ferroelectrics, magnetic semiconductors, systems with valence instabilities, magnetic and superconducting materials, heavy fermions, and, most recently, high-temperature superconductors.

Praveen Chaudhari *IBM Research Division, T. J. Watson Research Center, P.O. Box 218, Yorktown Heights, New York 10598.*
Dr. Chaudhari obtained a B.S.(Honors) from the Indian Institute of Technology (1961), and an M.S. (1963) and a Sc.D (1966), both in physical metallurgy, from the Massachusetts Institute of Technology, Cambridge. Since joining the T. J. Watson Research Center as a Research Staff Member in 1966, he has held various management responsibilities in science and science-related technologies such as optical storage, magnetic bubbles, and the Josephson program. He was appointed Director of the Physical Sciences Department in 1981, Vice-President for Science and Technology, IBM Research Division, in 1982, and a member of the Corporate Technical Committee in 1989. Dr. Chaudhari has worked on the structure and properties of amorphous solids, mechanical properties of thin films, defects in solids, quantum transport in disordered systems, superconductivity, and on the magnetic monopole and neutrino mass experiments. He has several IBM awards, and was the first recipient of the Leadership Award (1986) of the Metallurgical Society of AIME for his contributions to advancing the science and technology of electronic materials. He received the George E. Pake Award of the American Physical Society (1987) for his personal contributions to science and management of science. Dr. Chaudhari is a member of the American Association for the Advancement of Science, the American Institute of Mining, Metallurgical and Petroleum Engineers, and the National Academy of Engineering. He is a Fellow of the American Physical Society.

Christopher A. Feild *IBM Research Division, T. J. Watson Research Center, P.O. Box 218, Yorktown Heights, New York 10598.*
Mr. Feild joined the Physical Sciences Department of the T. J. Watson Research Center as an associate engineer in 1987. He received a B.S. in chemistry from Dickinson College, Carlisle, Pennsylvania, in 1986. Dr. Feild's interests include preparation, characterization, and electronic structure of unusual inorganic compounds. He is currently working on the synthesis and crystal growth of high-T_c superconductors.